Theor. Appl. Climatol. 85, 185–201 (2006)
DOI 10.1007/s00704-005-0178-4

Theoretical and Applied Climatology
Printed in Austria

[1] Urban Climate Group, Physical Geography, Göteborg University, Sweden
[2] Atmospheric Science Program, Department of Geography, Indiana University, Bloomington, IN, USA
[3] Environmental Monitoring and Modelling, Department of Geography, King's College London, London, UK

Longwave incoming radiation in the Tropics: results from field work in three African cities

P. Jonsson[1], **I. Eliasson**[1], **B. Holmer**[1], and **C. S. B. Grimmond**[2,3]

With 9 Figures

Received November 8, 2004; revised June 23, 2005; accepted July 3, 2005
Published online May 10, 2006

Summary

This study investigates differences in longwave incoming radiation ($L\downarrow$) within and between three African cities, Dar es Salaam (Tanzania), Ouagadougou (Burkina Faso), and Gaborone (Botswana), during the dry season, and evaluates the performance of a model to simulate these fluxes. In each city, direct observations of $L\downarrow$, shortwave incoming radiation ($K\downarrow$), air temperature, air humidity, and total suspended particle (TSP) concentration for three land uses (CBD, green residential, and traditional residential) were taken. The observed $L\downarrow$ flux decreases with increasing latitude, and temperature becomes an increasingly important factor in governing $L\downarrow$ variations further from the Equator. Humidity, as well as particle loading, differs significantly between the three cities. Differences between observed and modelled ε_{sky} for rural stations near all cities showed a clear diurnal variation, with maximum differences of 0.08 between day and night. This diurnal difference was incorporated in the model and, for urban areas the model overestimates $L\downarrow$ by around $25\,Wm^{-2}$. However, this model performs equally well regardless of the land use considered in any of the cities. The residual (difference between observed and modelled urban $L\downarrow$) did not show any correlation with particulate pollution. However, the difference between observed and calculated ε_{sky} is around 0.05 higher in Ouagadougou compared to the other cities, likely due to the heavy dust load observed here. It is concluded that tropical urban longwave radiation is not dramatically different from the mid latitudes.

1. Introduction

Incoming radiation fluxes play an important role in the surface energy balance in urban areas. The urban heat island (UHI), which is especially well developed during clear and calm nights, is closely linked to net longwave radiation at night (Oke and Fuggle, 1972; Nunez et al., 2000). At the surface of an urban area, longwave incoming radiation ($L\downarrow$) originates both from the sky and from objects obstructing the sky. In cities, vertical walls increase the area of radiating surfaces and energy is more effectively trapped and emitted compared to a flat surface of the same material (Aida, 1982; Arnfield, 1982). In general, $L\downarrow$ is considered to be higher in urban areas, both during day and night (Oke, 1997, p. 312). In addition to the effects of urban geometry/lower sky view factors, urban effects have been attributed to (1) a warmer urban atmosphere (e.g. Oke and Fuggle, 1972; Aida and Yaji, 1979; Estournel et al., 1983; Nunez et al., 2000); (2) higher emissivity brought about by a pollution layer (e.g. Rouse et al., 1973; Tapper, 1984; Miskolczi et al., 1997); and (3) higher moisture in the urban atmosphere (a more minor effect) (Holmer and Eliasson, 1999) (see summary in Table 1).

Table 1. Selected studies on $L\downarrow$ in urban areas in chronological order (see Table 4 for definition of symbols)

Reference	Lat.	Type of area	Type of study	Param.	Main conclusions
Oke and Fuggle (1972) *Montreal*, *Canada*	45° N	Urban/rural	Mobile measurements	$L\downarrow$, T_a	Urban $L\downarrow$ surplus can be explained by vertical temperature structure over the city alone without need to consider emissivity changes by pollution layer. Increased urban $L\downarrow$ is thus a result and not a cause of the UHI.
Rouse et al. (1973) *Hamilton*, *Canada*	43° N	Urban/rural	Stationary measurements	$L\downarrow$, $K\downarrow$	Urban particulate pollution plays a dual role in absorbing solar radiation and emitting infrared radiation.
Aida and Yaji (1979) *Tokyo*, *Japan*	35° N	Urban/rural	Mobile measurements	$L\downarrow$, T_a, q	Tokyo experiences 8–10% higher $L\downarrow$ on clear nights of which around 50% can be attributed to vertical temperature structure. Radiation inversions in rural areas decrease the difference as does less humidity in the city.
Estournel et al. (1983) *Toulouse*, *France*	44° N	Urban/rural	Stationary measurements	$L\downarrow$, $K\downarrow$	$L\downarrow$ higher in the city (15 $\mathrm{Wm^{-2}}$ at night, 25 $\mathrm{Wm^{-2}}$ in the afternoon) due to altered vertical temperature structure. The emissivity increase due to air pollution was very weak.
Tapper (1984) *Christchurch*, *New Zealand*	43° S	Urban/rural	Stationary measurements	$L\downarrow$	Comparison of observed ε with those calculated using Brutsaert's formula showed underestimation of the latter and is assigned to air pollution concentrations on sky ε.
Padmanabhamurty and Bandopadhyay (1994) *Delhi*, *India*	28° N	Urban/industrial/ suburban/rural	Stationary measurements	$L\downarrow$, $K\downarrow$, $L\downarrow$, $K\downarrow$, Q^*	$L\downarrow$ lowest at rural due to low levels of air pollutants, L highest at industrial site. $K\downarrow$ highest at rural because of lower air pollution concentrations.
Miskolczi et al. (1997) *Ilorin*, *Nigeria*	8° N	Suburban	Stationary measurements	$L\downarrow$	Minimum of $L\downarrow$ during Harmattan, combined effect of colder air and fewer clouds. The minimum is moderated by high content of Sahara dust.
Nunez et al. (2000) *Göteborg*, *Sweden*	57° N	Urban/rural/ intra-urban	Mobile measurements	$L\downarrow$, ψ_S	On average 11 $\mathrm{Wm^{-2}}$ higher $L\downarrow$ in the urban area due to vertical temperature structure. 20–30% of urban surplus is assigned to aerosols. Good relationship found between $L\downarrow$ and SVF ($R^2 > 0.9$).

To date, few studies have been conducted which focus on longwave radiative fluxes in tropical urban areas, despite the large and increasing number of people who live in cities at these latitudes (Jauregui, 1999). One exception is the work conducted by Padmanabhamurty and Bandopadhyay (1994) who measured $L\downarrow$ fluxes for four different land uses (rural, commercial, residential and industrial) in Delhi. Their study revealed differences within the city; the highest values of $L\downarrow$ were observed at the industrial site together with an old commercial area. A higher atmospheric temperature associated with these landuses, attributed to the presence of pollutants, was proposed as an explanation. In a different study, Miskolczi et al. (1997) reported results from two years of continuous measurements of $L\downarrow$ at a Nigerian university campus in sub-Sahel Africa. The minimum $L\downarrow$ occurred during the Harmattan season (the period when the dusty northerly winds blow from the Sahara) due to the combined effect of lower air temperatures and the higher atmospheric transparency associated with lower cloud cover. However, the Harmattan was believed to have had a moderating effect on the minimum. Estimates of the effects of dust loading for a standard air column over the Sahara, under clear sky conditions, (Claquin et al., 1998), suggest a forcing effect of 48 Wm^{-2} on the longwave incoming radiation (Table 1).

The extreme humidities, both low and high, found in the Tropics exceed those of mid-latitude cities. The wet Tropics in Equatorial areas are likely to have unstable and moist atmospheres and thus the $L\downarrow$ flux is influenced by high humidity. In the dry Tropics, in contrast, the high stability and associated surface inversions at night, plus dusty environments, will impact $L\downarrow$. Coastal locations will exhibit yet another regime with sea and land breeze episodes and better ventilation of air masses. Finally, the structure of cities in tropical areas, especially in African cities south of the Sahara, tends to be more open than at higher latitudes which has implications for $L\downarrow$.

The aim of this study is to investigate the longwave incoming radiation flux between and within cities in tropical environments. Three African cities (Dar es Salaam, Tanzania; Ouagadougou, Burkina Faso; and Gaborone, Botswana) were chosen in order to study cities of different sizes within in a range of latitudes and physical settings. Models of $L\downarrow$ are also evaluated. Particular attention is directed to the role of suspended particulate matter, atmospheric humidity, and urban structure on the longwave incoming radiation.

2. The study areas

Africa is a predominantly dry and rural continent with a rapid rate of urbanization (Cohen, 2004). Thus, the main source of particulate air pollution is soil derived dust. In many African cities air pollution is neither monitored nor controlled, and there are no long term records of pollution levels and impacts (Fenger, 1999). Major differences in anthropogenic air pollution between Africa and the industrialized world exist. In Africa, biomass burning (bush fires and fuel wood consumption, which accounts for 80% of the total energy use in sub-Sahara Africa) is a major source of pollutants (World Bank, 1996).

Climatically, Africa is symmetrically located around the Equator (Cape Blanc 37° N, Cape Agulhas 35° S) with the effect that climatic zones on both sides of the Equator are more or less mirror images. Mountain ranges that act as climate barriers in other parts of the world, such as the Andes and the Rocky Mountains, are largely absent in Africa. Subtropical high pressure cells are therefore free to reign and generate vast dry areas (Trewartha, 1982, p. 91).

The three cities studied, in order of descending population and increasing distance from the Equator, are Dar es Salaam, Ouagadougou, and Gaborone (Fig. 1). Details on each are provided below and in Table 2.

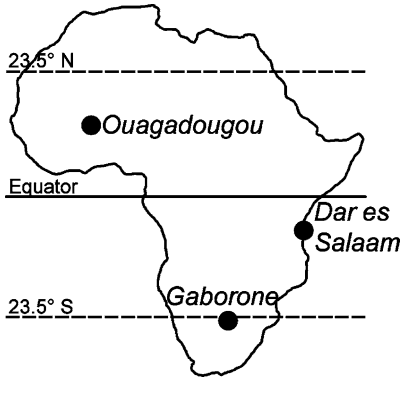

Fig. 1. The locations of the three cities

Table 2. Overview of city characteristics

	DAR ES SALAAM *Tanzania*	OUAGADOUGOU *Burkina Faso*	GABORONE *Botswana*
Location	Coastal	Inland	Inland plateau
Lat, long	6°51′S, 39°18′E	12°20′N, 1°40′W	24°40′S, 25°55′E
Population 2003[1] ($\times 10^6$)	2.44	0.82	0.20
Status of road network	Few ring roads, congestion in centre common. Roads are paved unless within residential areas.	All centre roads are paved, in traditional residential areas dirt roads prevail.	Almost all roads are paved.
Mean monthly temperature (°C) (left y-axis) and precipitation (mm) (right y-axis)[2]	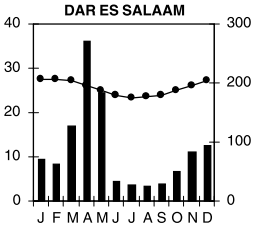	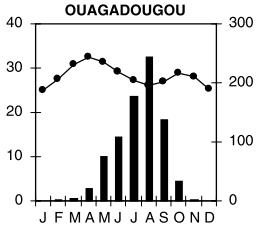	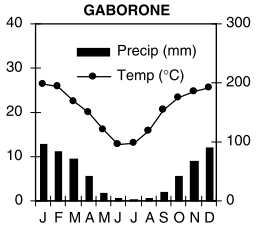

Sources: [1] United Nations, 2004; [2] Worldclimate, 2005

2.1 Dar es Salaam, Tanzania

Dar es Salaam (Fig. 1) is located on a coastal flat, bounded by the Indian Ocean to the east and the Pugu hills to the west. Currently, the population of the Dar es Salaam region is estimated to be 2.44 million (United Nations, 2004). The city has sub-centers that are divided by great distances from each other and from the Central Business District (CBD). Within Dar es Salaam there is a small CBD with approximately 10 buildings of 10 or more storeys. The rather small city centre is mostly a commercial area, while the bulk of the population lives in suburbs. Thus, most commuters travel to the city centre generating high levels of traffic congestion.

The regional climate of the Dar es Salaam area is hot and humid with an annual rainfall of 1050 mm (Table 2). The mean temperature is 26 °C and there is only a slight seasonal variation in temperature due to the city's proximity to the Equator (Woodlock, 1974, p. 84). Average relative humidity ranges between 96% in the morning to 67% in the afternoon (Kimaryo, 1996). The general circulation is characteristically monsoonal due to the passage of the Inter-Tropical Convergence Zone. Two seasons can be distinguished: the SE monsoon between April and October, and the NE monsoon between October and March (Trewartha, 1982, p. 124). As Dar es Salaam is a coastal location, the near surface winds are modified by land and sea breezes. Mbuligwe and Kassenga (1997) suggest that Dar es Salaam has a significant air pollution problem because of the high concentration of passenger vehicles in a relatively small area of closely spaced buildings, which hinder the dispersion of pollutants.

2.2 Ouagadougou, Burkina Faso

Ouagadougou, capital of Burkina Faso, has a population of approximately 0.8 million (United Nations, 2004) and like Dar es Salaam it is spread out with a rather small, but busy, centre. The city lies in flat surroundings at an altitude of approximately 300 m a.s.l. Different types of residential area can be found, ranging from wealthy to very poor and simple. In the latter area, streets are not paved and facilities for water and waste do not exist. In the outskirts of the city, unplanned settlements grow rapidly, especially along the major roads around the city (Offerle et al., 2005). For example, the airport was located outside the city limits in the 1980s but is now in the central part of the city. The other prominent city features are the several reservoirs that divide northern areas from the city centre.

The climate of Ouagadougou has distinct seasons. Although located close to the Sahara, precipitation levels are fairly high with an annual rainfall of around 800 mm. Almost all

of this rain falls in the summer months of May through September, while the remainder of the year is dry (Table 2). Consequently, the winter months are dusty, due both to dry soil surfaces and also because of the northerly winds, Harmattan, which bring dust from the Sahara. The air pollution situation in Ouagadougou is severe. Poor air quality can be smelled and seen. In addition to the dusty ambient environment, the common use of light motorcycles that run on heavy oil mixed fuel, which usually contains twice the recommended percentage of oil (Diallo, 2004), amplifies the situation. Stable atmospheric conditions during the winter months, especially at night, lead to the weak dispersion of pollutants.

2.3 Gaborone, Botswana

The city of Gaborone has roughly 200,000 inhabitants (United Nations, 2004) and is situated in the southeastern part of Botswana some 100 km south of the Tropic of Capricorn (Fig. 1). Botswana is located on a plateau and the capital city, Gaborone, is elevated about 1000 m a.s.l. The topography ranges from undulating to flat, with elevational differences of approximately 50 m. The majority of the residential areas are one storey houses and resemble a suburb. Only in the small CBD are there buildings of 5–10 storeys in height.

The climate of the Gaborone region is influenced by the subtropical high-pressure belt, yielding dry winters with a large daily temperature range and rainier summers (Table 2). Precipitation during summer is associated with the movement of the Inter-Tropical Convergence Zone. Gaborone has a mean annual temperature of 20.7 °C and a mean annual precipitation of 540 mm (Climatological summaries for Botswana, Department of Meteorological Services, 1984). Of this rainfall, 84% falls from October to the beginning of April, suggesting that clear skies are predominant during the rest of the year.

A few studies focussing on air pollution in Gaborone have been conducted. Of particular interest here are the measurements of Jayaratne and Verma (2001) of particle concentrations for different seasons. They found that particle concentrations were notably higher during winter than during the summer.

3. Methods

The following section describes the measurement procedures for $L\downarrow$, $K\downarrow$, temperature, relative humidity and total suspended particles (TSP) in the three cities. This is followed by a description of how the data were analysed. Finally, the construction of a $L\downarrow$ model for urban areas is presented.

3.1 Sampling strategy

In each of the three cities, three land uses, that were considered to represent the diversity of land cover, were sampled: the central business district (CBD); a traditional residential area; and a wealthier residential area, which is typically more highly vegetated. The residential areas differ between the cities with respect to the standard of living (e.g. waste disposal, electricity, sewage, street illumination, vegetation density and irrigation). To provide a reference for each of the cities, a control station was set up in an unhabitated area, referred to hereafter as rural.

In each of the three areas, ten (Ouagadougou, Gaborone) and twelve (Dar es Salaam) measurement points were identified with approximately half at road intersections and the remainder mid-block. These points covered an area of approximately 0.16 km^2 in Dar es Salaam, 0.15 km^2 in

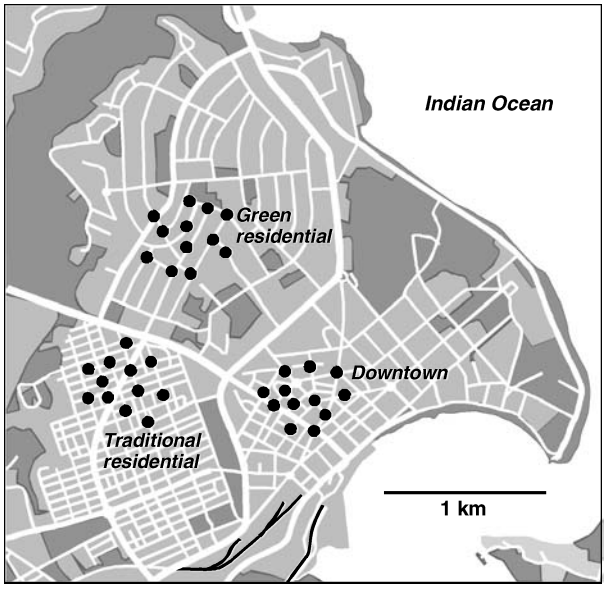

Fig. 2. The three different areas of Dar es Salaam with the points of measurement marked. The areas in Ouagadougou and Gaborone are of similar size

Table 3. Length of field work periods, number of sites in each area, and number of cloud-free morning (*MO*) noon (*NO*) and night (*NI*) measurements

City	Period	Sites/area	CBD			Green residential			Traditional residential		
			MO	*NO*	*NI*	*MO*	*NO*	*NI*	*MO*	*NO*	*NI*
Dar es Salaam	Oct. 1–24 2002	12	2	1	4	2	1	1	1	–	3
Ouagadougou	Feb. 13–25 2003	10	1	2	2	2	2	1	2	2	1
Gaborone	Sep. 9–20 2003	10	2	1	1	2	3	2	1	2	2

Ouagadougou, and 0.10 km^2 in Gaborone for each land use. Figure 2 shows a schematic map of central Dar es Salaam and the three areas of measurements as an example of the sampling pattern. In Ouagadougou the areas were further apart than in Dar es Salaam and Gaborone, but it was considered more important to include the range of urban land uses and morphologies rather than to have a high density of measurement points.

Measurements were conducted on three week days in each area. In Dar es Salaam an additional day of measurements was required for each area in order to capture totally cloudless conditions. Table 3 shows the total number of samples for each location under cloudless conditions. Measurements for an area were taken throughout a specific day. A route that passed through all points in each area was selected. Measurements began at 0700 h local time (early morning, beginning of rush hour), 1100 h (close to solar noon), and 1900 h (after sunset). Each measurement transect was completed in 1–1.5 h depending on traffic. It took 5 minutes to carry out measurements at each point.

3.2 Measurements and equipment

A set of instruments were mounted on the roof of a car to measure $L\downarrow$ (Kipp & Zonen CG 1 pyrgeometer), $K\downarrow$ (Kipp & Zonen CM 3 pyranometer), temperature/relative humidity (shielded Rotronic sensor), and total suspended particles (TSP) (MetOne Aerocet 531 particle counter). The pyrgeometer and pyranometer were fixed to an adjustable camera tripod head that was mounted on the car roof to allow the instrument to be levelled at each point. The pyrgeometer, pyranometer and the temperature/relative humidity sensor were sampled at 0.1 Hz, and 1 min averages were recorded onto a Campbell Scientific CR 10 data logger. The particle counter sampled every 2 min yielding two values of TSP in mg m^{-3} at each point. This device was placed on the roof of the car at each stop. At each point, cloud cover observations were also made.

At the rural reference stations of all cities, an identical set of instruments were installed together with a sonic anemometer (GILL Wind Master Pro). The instruments sampled $L\downarrow$, $K\downarrow$, temperature/relative humidity, as well as wind speed and direction at 0.1 Hz. Ten minute averages were recorded onto a Campbell Scientific CR 10 data logger. The particle counter sampled TSP concentration every 2 min. The anemometer was mounted at 3 m and the other instruments on a tripod at 1.7 m.

In order to determine the degree of sky obstruction at each point, sky view factor (SVF) photographs were taken with a fisheye lens and digital camera from the car roof (at approximately 1.7 m height). The camera was fixed on the tripod, allowing the camera to be levelled at each point. For the Ouagadougou digital images, a SVF method developed by Grimmond et al. (2001) was used, while a method developed by Holmer et al. (2001) was used to analyse the analog images from Dar es Salaam and Gaborone.

3.3 Data

For each observation point, 5 min averages (4 min for particulate data) for each variable were determined. Given the influence of cloud cover on $L\downarrow$, only cloud-free episodes were considered (Table 3).

For the rural stations in each city, data from cloudless 24 h periods (2 in Dar es Salaam, 3 in Ouagadougou, and 3 in Gaborone) were removed from the full data set. To account for the pyrgeometer dome heating effect on the $L\downarrow$ measurements during sun lit hours, 0.025 $K\downarrow$ (25 Wm^{-2} per 1000 Wm^{-2}) was subtracted from the observed values of $L\downarrow$ based on the pyrgeometer manual (Kipp and Zonen, 2002).

3.4 Estimation of longwave radiation and emissivities

Longwave incoming radiation received at the surface depends on the vertical distribution of water vapour, carbon dioxide, ozone, atmospheric aerosols and the vertical profile of temperature. However, data presented here are derived from near surface observations of temperature and humidity.

The sky emissivity, that is the driving force behind a change in $L\downarrow$ when temperature is held constant and the sky view factor (ψ_S, SVF) is set to 1, can be estimated using several formulae. Commonly cited equations are those of Brunt (1932), Swinbank (1963), Idso and Jackson (1969), Brutsaert (1975), and Idso (1981). Prata (1996) has described these as limited since they are based on measurements that were unreliable under strong insolation and because of their small geographical extent. Prata's (1996) formulation for sky emissivity, based on 4600 radiosonde profiles, relates the vertical distribution of temperature and precipitable water to screen level observations. It is considered by Offerle et al. (2003), based on Newton (1999) and other studies, to have the best performance.

For a location with $\psi_S = 1$ under clear sky conditions, the $L\downarrow$ (Wm^{-2}) is given by the Stefan Bolzmann's law:

$$L\downarrow = \varepsilon_{\mathrm{sky}}\sigma T_a^4 \tag{1}$$

where $\varepsilon_{\mathrm{sky}}$ is the atmospheric emissivity, σ the Stefan Bolzmann's constant ($5.67 \times 10^{-8}\,\mathrm{Wm}^{-2}\,\mathrm{K}^{-4}$), and T_a the air temperature (K). When the $\psi_S < 1$, as it is in urban environments, the emissivity of wall materials (ε_w) need to be estimated. Examples of typical values are given by Oke (1987): glass has an emissivity of 0.87–0.94; brick 0.90–0.92; and deciduous vegetation 0.97–0.98. Further, Harman et al. (2004) have suggested that urban energy models based on the urban canyon need to consider at least one reflection of longwave radiation. Neglecting the effect of reflections would yield large errors. Therefore, for a location with sky obstruction ($\psi_S < 1$), based on Nunez et al. (2000) and Harman et al. (2004), the following is used:

$$L\downarrow = \left[\psi_S\varepsilon_{\mathrm{sky}}\sigma T_a^4\right] + \left[(1-\psi_S)\varepsilon_w\sigma T_w^4\right] + \left[(1-\psi_S)(1-\varepsilon_w)\varepsilon_{\mathrm{sky}}\sigma T_a^4\right] \tag{2}$$

where T_w is the wall temperature (K). The first term on the right-hand side is the direct sky longwave radiation, the second is the wall radiation, and the third is the reflected sky radiation.

Thus, in cases where $L\downarrow$ is observed, the atmospheric emissivity can be estimated ($\hat{\varepsilon}_{\mathrm{sky}}$) as follows:

$$\text{if } \psi_S = 1 \quad \hat{\varepsilon}_{\mathrm{sky}} = L\downarrow_{\mathrm{obs}}/\sigma T_a^4 \quad \text{or} \tag{3}$$

$$\text{if } \psi_S < 1 \quad \hat{\varepsilon}_{\mathrm{sky}} = \frac{L\downarrow_{\mathrm{obs}} - (1-\psi_S)\varepsilon_w\sigma T_w^4}{[\psi_S + (1-\psi_S)(1-\varepsilon_w)]\sigma T_a^4} \tag{4}$$

For urban areas, a sensitivity test was performed to investigate the importance of changing ε_w and T_w to $\hat{\varepsilon}_{\mathrm{sky}}$. Nine cases with different assumptions of ε_W and T_w were made for each area. For T_w, wall surface temperature measurements made in Ouagadougou by Offerle et al. (2005) were used as guidance when these assumptions were made. For the first case, $T_w = T_a$ for all areas was assumed. In the second case, CBD average wall surface temperatures were assumed to be 1.4 K warmer than T_a at morning, noon, and night. For the green residential area, $T_w = T_a$ was assumed and for the traditional area $T_w = T_a + 3.5$ K for all times of the day. In the third case, wall surface temperatures used in case 2 were increased by 2 K for all areas and times. For ε_w, the following assumptions were made according to the visual inspection of dominant materials in each area and their respective emissivities based on Oke (1987). In the CBD, green, and traditional areas of all cities, values of $\varepsilon_w = 0.85 \pm 0.03$, $\varepsilon_w = 0.95 \pm 0.03$, and $\varepsilon_w = 0.90 \pm 0.03$ were assigned, respectively. Since the nine different cases showed little variation in $\hat{\varepsilon}_{\mathrm{sky}}$, the nine different $\hat{\varepsilon}_{\mathrm{sky}}$ were used when $L\downarrow$ was calculated. The average of the nine different model results was accepted as the best value and is presented in the results section.

To calculate clear sky emissivity ($\varepsilon_{\mathrm{sky\,mod}}$), both rural and urban, the Prata (1996) formulation was used:

$$\varepsilon_{\mathrm{sky\,mod}} = 1 - \left(1 + 46.5\frac{e_a}{T_a}\right) \times \exp\left[-\left(1.2 + 3.0 \times 46.5\frac{e_a}{T_a}\right)^{0.5}\right] \tag{5}$$

where e_a is the vapour pressure (hPa). To check the performance of (6) in this region the clear sky emissivity model by Garratt (1992) was tested, as this was found to have the most reliable performance by Finch and Best (2004):

$$\varepsilon_{\text{sky mod}} = 0.79 - 0.174\exp(-0.095e_a) \quad (6)$$

For high-altitude sites, Prata (1996) proposed a correction since the vertical column of air affecting the emissivity is less:

$$\Delta\varepsilon_{\text{press}} = -0.05(1013.25 - P_{\text{site}})/(1013.25 - 710) \quad (7)$$

where P_{site} is the station level air pressure (hPa). As daily air pressure is not available, averages are used: 978 hPa in Ouagadougou, and 904 hPa in Gaborone. These result in corrections of -0.018 and -0.006, respectively. In the calculations of $L\downarrow$, with Eq. (4), the Prata formulae in Eqs. 3 and 7 were used for ε_{sky}.

Multiple regression was used to identify the importance of temperature, specific humidity (q), sky view factor (ψ_S), and TSP on variations in $L\downarrow$. To assess significant differences between the areas of each city, analysis of variance (ANOVA) was performed.

4. Results

First the magnitudes of the measured parameters in all cities and their land uses are presented. The data from urban and rural areas are used to compare modelled and observed emissivities. These emissivities are used to model $L\downarrow$ and discrepancies between observed and modelled $L\downarrow$ are correlated with levels of TSP.

4.1 Observed values of all parameters – inter-urban differences

The mean and standard deviations from all mobile measurements made during cloudless conditions are shown in Fig. 3. Note that there was no occasion of totally cloud-free conditions in the traditional residential area of Dar es Salaam at noon (Table 3). Also, it should be remembered that the measurements were conducted on different days and the only meteorological parameter that is held constant here is cloud cover. Data from the rural sites are not included due to instrumentation malfunction.

Dar es Salaam has, on average, the highest values $L\downarrow$, followed by Ouagadougou and Gaborone at all times. The average TSP concen-

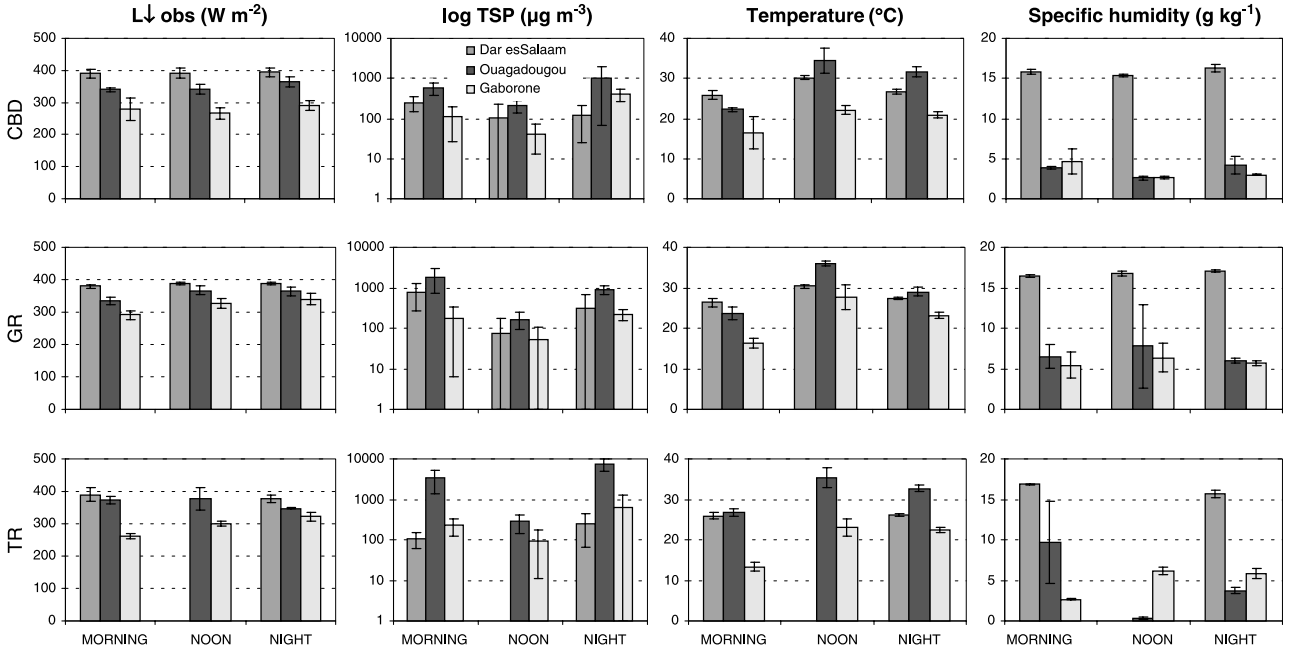

Fig. 3. Mean observed data from mobile measurements made during cloudless conditions in central business district (CBD), green residential (GR) and traditional residential (TR) areas. See Table 3 for N for each set. Standard deviation is given by the error bars

tration, for all times and areas, is greatest in Ouagadougou (1750 $\mu g\,m^{-3}$), followed by Dar es Salaam (250 $\mu g\,m^{-3}$), and Gaborone (220 $\mu g\,m^{-3}$) (Fig. 3). The differences between Ouagadougou and the other cities are large. However, the diurnal pattern of all cities is similar, with morning and night maxima, while concentrations during midday are fairly similar for all cities and are relatively low compared to other periods of the day.

Ouagadougou was the warmest of the cities during the field campaigns with hot days and mild mornings and nights (Fig. 3). Dar es Salaam is second warmest and due to its coastal location the diurnal temperature range is small. Small standard deviations further indicate the small variations in temperatures from day to day. The air temperatures in Gaborone were rather low, as expected for the winter season measurements. As in Ouagadougou, Gaborone temperatures were more variable as confirmed by higher standard deviations.

As would be expected, due to its oceanic location close to the Equator, Dar es Salaam has the highest specific humidity and the smallest diurnal variation (Fig. 3). Dar es Salaam also experiences very little variation in air humidity illustrated by the very small standard deviations. The lower humidities measured in Ouagadougou and Gaborone are easily explained by the proximity of each of these cities to arid environments. The higher variability in Gaborone and Ouagadougou is due to intrusions of different air masses.

To investigate which variable, temperature (T_a), specific humidity (q), ψ_S and TSP, has the greatest influence on $L\downarrow$ variations, multiple stepwise regression analysis was performed. Table 4 shows results from this analysis, statistically significant at the 5% level. Results based on Dar es Salaam data show ψ_S to be the most important parameter in accounting for variation in $L\downarrow$, followed by q, and T_a. In Ouagadougou, q has the greatest influence, followed by T_a and ψ_S. Note that TSP does not make a significant contribution to $L\downarrow$ in Ouagadougou. In Gaborone, temperature was the most influential variable on $L\downarrow$, followed by q and ψ_S. Interestingly, TSP has a significant effect on $L\downarrow$ here. The accumulated explained variance for all parameters is 76% in Dar es Salaam, 81% in Ouagadougou, and 64% in Gaborone.

Table 4. Accumulated explanation from multiple step-wise regression of all data with $\geq$0.05 significance level. $L\downarrow$ is dependent factor and air temperature (T_a), specific humidity (q), sky-view factor (ψ_S) and total suspended particulate matter (TSP) are independent factors

Step/number of importance	Dar es Salaam		Ouagadougou		Gaborone	
1	ψ_S	0.50	q	0.31	T_a	0.44
2	q	0.70	T_a	0.56	q	0.59
3	T_a	0.76	ψ_S	0.81	ψ_S	0.62
4	–	–	–	–	TSP	0.64

4.2 Intra-urban differences

At an intra-urban scale, $L\downarrow$ in Dar es Salaam varies least between the different land uses. In the CBD and in the green residential area there is almost no variation through the day and standard deviations in these areas are small, indicating that the $L\downarrow$ flux is stable. As data are missing in the traditional residential area, it is harder to draw firm conclusions for this site. In Ouagadougou and Gaborone, the intra-urban variance is larger with the CBD having the smallest fluxes. Standard deviations vary more in these two cities than in Dar es Salaam.

The busy CBD area in each of the cities does not display the highest TSP levels as might have been expected. In Dar es Salaam, it is actually the green residential area that exhibits the highest concentration. In both Ouagadougou and Gaborone, the traditional residential areas are most heavily polluted with particulate matter. Ouagadougou experienced astonishing concentrations on average of 3350 and 7470 $\mu g\,m^{-3}$ in the morning and night, respectively, in this area.

Intra-urban temperature differences in Dar es Salaam are small with highest temperatures recorded in the green residential area. In Ouagadougou and Gaborone, the more traditional residential areas are the warmest. Humidity differences within Dar es Salaam are negligible. The CBDs in Ouagadougou and Gaborone have significantly lower humidity than the traditional residential areas, while the green areas are most humid. An analysis of variance is shown in Table 5. In Dar es Salaam the CBD-area has significantly higher $L\downarrow$ and in Ouagadougou the traditional residential area has lower $L\downarrow$ while in Gaborone all three areas differ.

Table 5. Statistically significant intra-urban differences in longwave incoming radiation (Wm^{-2}) based on ANOVA

Subset	Dar es Salaam		Ouagadougou		Gaborone	
	Area	*Average L↓*	*Area*	*Average L↓*	*Area*	*Average L↓*
1	Trad	380	Trad	350	CBD	280
	Green	386				
2	CBD	393	CBD	363	Trad	301
			Green	367		
3	–	–	–	–	Green	320

Table 6. Mean sky view factors in all areas of each city

	CBD	Green residential	Traditional residential
Dar es Salaam	0.59	0.81	0.75
Ouagadougou	0.80	0.82	0.93
Gaborone	0.80	0.73	0.81

Dar es Salaam is the city with the lowest ψ_S in the CBD and is the study site with the densest urban structure (Table 6). Ouagadougou and Gaborone have approximately the same CBD urban density. In the green residential areas most sky obstructions result from vegetation. In Gaborone the vegetation is so dense in the green residential area that it has the lowest ψ_S, while the corresponding area in Dar es Salaam has the highest ψ_S. The traditional residential areas are less vegetated and have highest ψ_S in both Ouagadougou and Gaborone.

4.3 'Observed' emissivities

Figure 4 shows the emissivities estimated from the rural stations (Eq. 3) together with those from the urban sites in each city (Eq. 4). Note that for the rural stations only observations from times corresponding to the morning, noon and night measurements in the urban areas are presented. The urban sites show greater scatter in their emissivities. The averages of these observations show that all rural stations have higher emissivities than their urban counterparts by 0.03.

Figure 5 shows the intra-urban averages of these observations and the diurnal mean for the rural sites. It shows that urban sky emissivities are lower in all three cities, with Ouagadougou in the morning being the only exception. What is clear is that there is not a distinct pattern related to land use. The rural stations have a marked diurnal variation in sky emissivity, with lower values occurring during the daytime.

4.4 Modelled emissivities

The difference between observed and modelled emissivity ($\Delta\varepsilon_{\mathrm{sky}}$) for rural (Eqs. 3 and 5) and urban (Eqs. 4 and 5) sites are shown in Fig. 6. At the rural sites for all three cities, the diurnal pattern is similar to that of observed emissivity

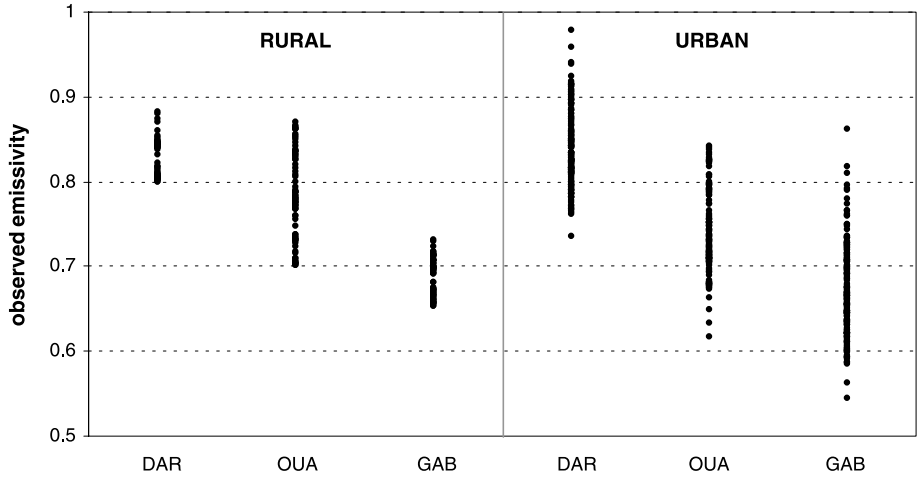

Fig. 4. Observed sky emissivity at the rural and urban sites in each city. Only observations corresponding to morning (0700–0830 h), noon (1100–1230 h) and night (1900–2030 h) measurements are shown

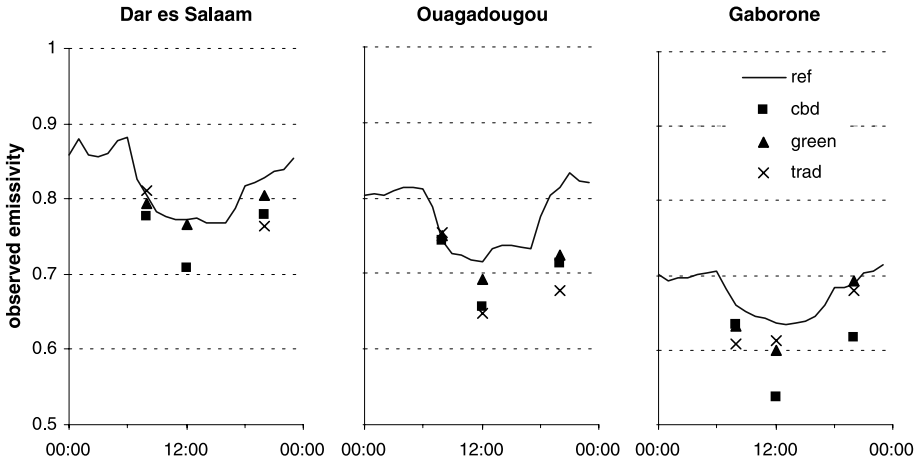

Fig. 5. Mean observed sky emissivities for rural (ref) and urban (cbd, green, trad) sites of each city

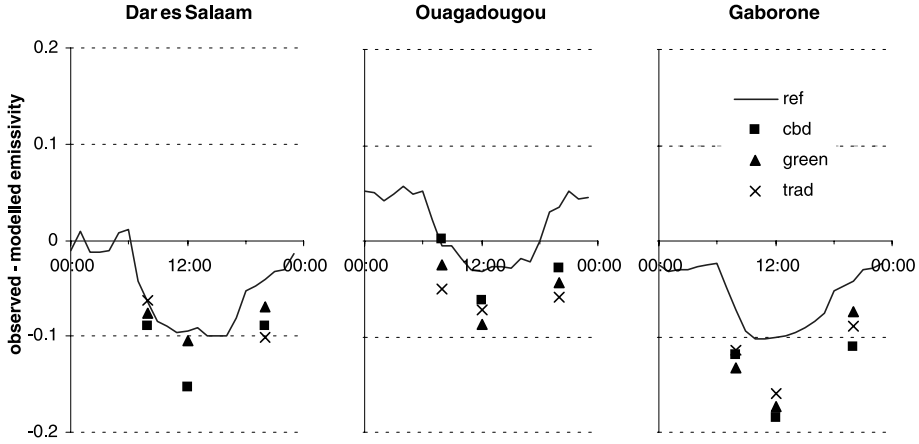

Fig. 6. Differences between observed and modelled emissivity ($\Delta\varepsilon_{sky}$) (using Prata formula) for all areas in each city

shown in Fig. 5. The Prata formulation takes humidity and temperature variations into account and thus the diurnal pattern is most probably due to the near surface temperature and humidity profiles. In Ouagadougou $\Delta\varepsilon_{sky}$ is positive, while for Dar es Salaam and Gaborone it is negative (Fig. 6). Thus, Prata underestimates during mornings and nights in Ouagadougou. The different land uses in the cities show no detectable pattern in emissivity differences.

When the mean $\Delta\varepsilon_{sky}$ for each site is subtracted, so values are centred on 0, the diurnal pattern is very similar (Fig. 7). The difference of 0.04 between $\varepsilon_{sky\,obs}$ and $\varepsilon_{sky\,mod}$, as is shown

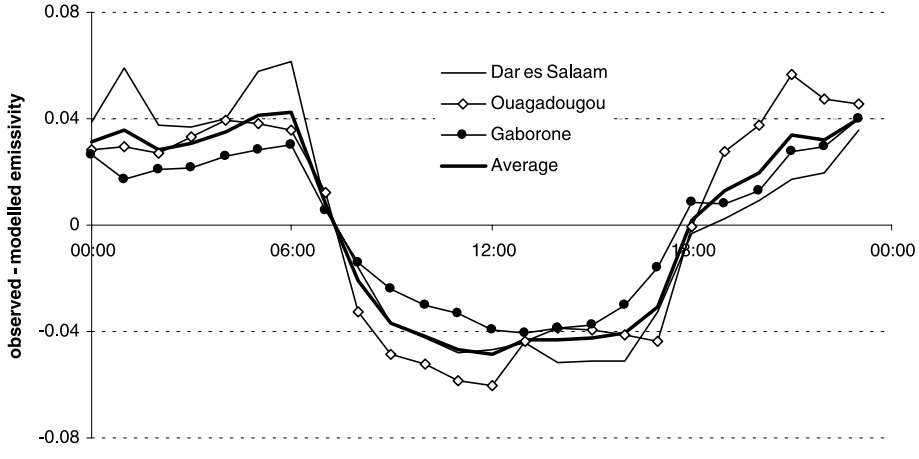

Fig. 7. Differences between observed and modelled emissivity (using the Prata formulation) at the rural sites centred on 0

in Fig. 7 around noon, would yield a change of approximately 20 Wm^{-2} in $L\downarrow$. The Garratt formulation of $\varepsilon_{\mathrm{sky\,mod}}$ (Eq. 6) showed strikingly similar results.

4.5 Performance of modelled $L\downarrow$ with single reflection

Given ψ_S, and making assumptions about wall surface temperatures (see Section 3.4.) and emissivities, it is possible to model $L\downarrow$ in urban areas using Eq. 2. Figure 7 showed that during the morning (0700–0830 h) and night (1900–2030 h) measurements there is no need to correct the Prata formula (difference between observed and modelled $\varepsilon \approx 0$). At noon (1100–1230 h) the Prata formula overestimates by approximately 0.04 and thus this quantity should be subtracted from $\varepsilon_{\mathrm{sky\,mod}}$ in Eq. (5) for noon measurements. Figure 8 shows the results for all data (Fig. 8a), by city (Fig. 8b), by land use (Fig. 8c), and by time of day (Fig. 8d).

The model does a fairly good job when all data (Fig. 8a) are included with an explained variance of 0.88, although it overestimates $L\downarrow$. The model performs best in Ouagadougou ($R^2 = 0.77$) despite the extreme particle concentrations observed here (Fig. 8b). In both Dar es Salaam and Gaborone the explained variances are slightly lower ($R^2 = 0.69$ and 0.71, respectively). In Fig. 8c, where the data set is stratified by land use, it is evident that the model performs best in the CBD and traditional residential area ($R^2 = 0.90$ and 0.89, respectively), while performance is poorest in the green residential area ($R^2 = 0.83$). However, the slopes of the best fit trend lines are very similar. This is also the case regarding the different times of the day (Fig. 8d).

4.6 The particulate matter paradox

The difference between modelled and observed $L\downarrow$ is shown in Fig. 9a along with observed $L\downarrow$. On average, the model overestimates by

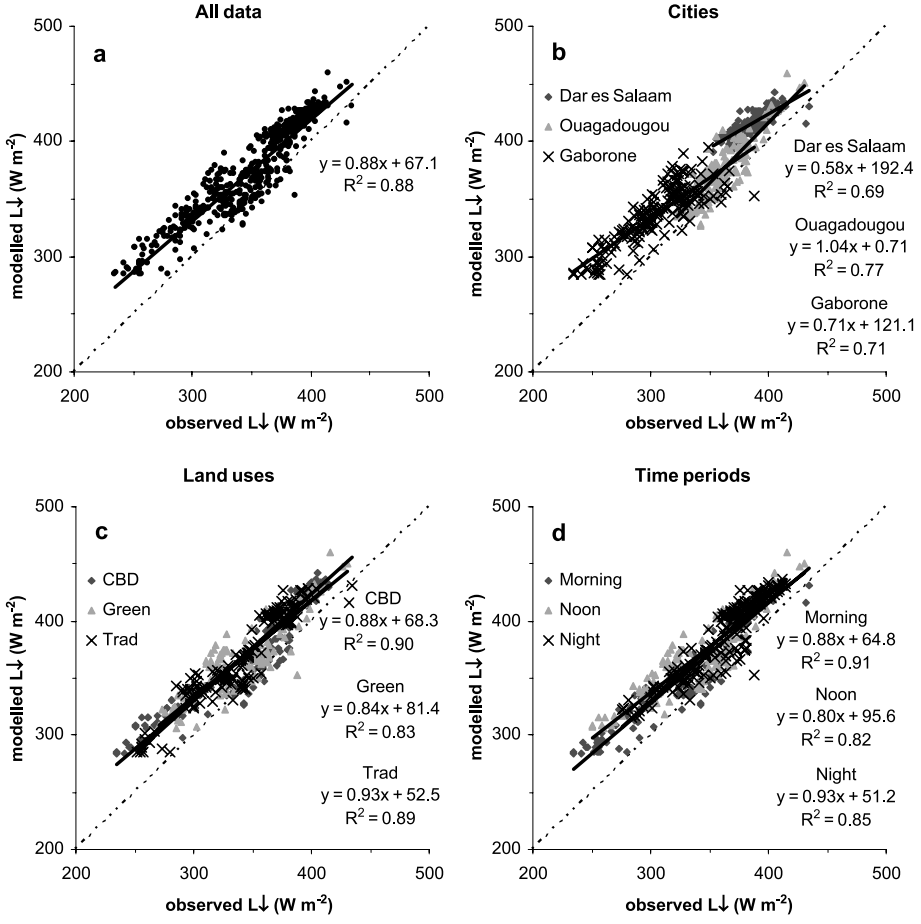

Fig. 8. Observed and modelled $L\downarrow$ with a single reflection for (**a**) all data, (**b**) each city, (**c**) each land use, and (**d**) each time of the day. Noon measurements have been corrected ε by −0.04 in all graphs

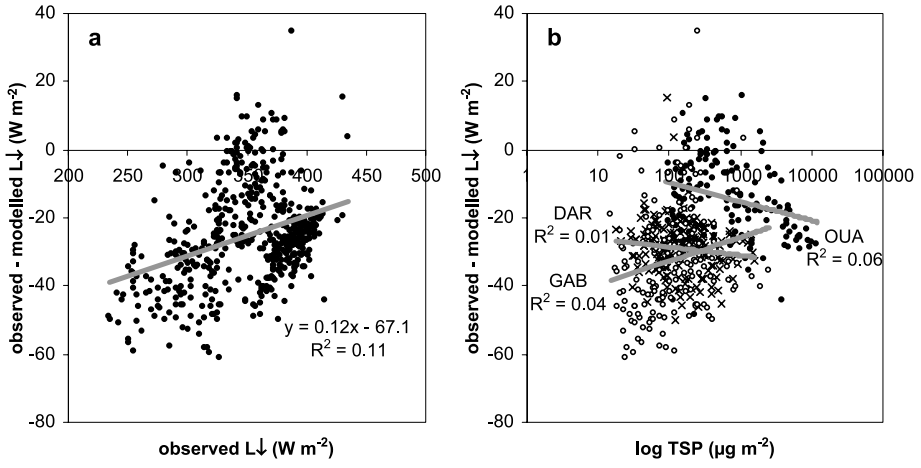

Fig. 9. Difference between observed and modelled $L\downarrow$ plotted with **a**) observed $L\downarrow$ for all urban data and **b**) with log TSP

$25\,\mathrm{W m^{-2}}$. The overestimation becomes larger at smaller observed values of $L\downarrow$. Prata (1996) found the same relation, suggesting this is part of $\varepsilon_{\mathrm{sky}}$ calculation.

A priori it may have been expected that the difference between modelled and observed $L\downarrow$ may be related to TSP. However, the influence of particles has not been found to be straightforward in this study. In Ouagadougou, the city with the greatest concentrations of TSP, the rural $\Delta\varepsilon_{\mathrm{sky}}$ was positively displaced compared to the other cities, indicating that the Prata formula underestimated $\varepsilon_{\mathrm{sky}}$ at times of high TSP (Fig. 6). However, Fig. 9b shows no coherent relation between the $\Delta L\downarrow$ residual and log TSP in the three cities. Thus, the overestimation of the model appears not to be related to TSP at ground level. It is surprising, given the wide range of TSP levels reported here (up to $7500\,\mu\mathrm{g\,m^{-3}}$), that this does not seem to have an influence on $L\downarrow$. Previous studies, for example Tapper (1984), have found a linear relationship between $L\downarrow$ and log TSP, albeit with smaller TSP concentrations.

5. Discussion

5.1 Inter- and intra-urban differences of $L\downarrow$

Temperature, sky obstruction, air pollution and humidity are, as described above, factors that govern longwave incoming radiation in the urban canopy layer. Data from Dar es Salaam showed the highest average values of $L\downarrow$ which can be attributed to high temperatures and high overall humidity. In Gaborone the lower absolute values of $L\downarrow$ can be attributed to the higher altitude which moderates both temperatures and humidity. The $L\downarrow$ values for Ouagadougou fall in between that of the other two cities in spite of the very high load of TSP (the highest concentrations at all times in all areas; $1750\,\mu\mathrm{g\,m^{-3}}$ on average) and the highest temperatures. The fact that Ouagadougou, on many occasions, was the driest city, again illustrates the important influence of humidity on $L\downarrow$.

With respect to intra-urban differences, the CBD of Dar es Salaam has the highest $L\downarrow$ flux. The low average ψ_S probably plays an important role (Table 5) as argued by Nunez et al. (2000). In Ouagadougou, the highest $L\downarrow$ fluxes were observed in the green residential area. The traditional residential area also showed similar to or higher values than those found at the CBD. In Gaborone, the green residential and traditional residential areas showed higher $L\downarrow$ flux than the CBD. Both Ouagadougou and Gaborone have lower ψ_S in the residential areas than in the CBD areas, in contrast to Dar es Salaam (Table 6). In Gaborone, the average ψ_S of the green residential area is actually lower than that of the CBD and since vegetation (the dominant sky obstruction in the area) has higher emissivity (Oke, 1987), a higher $L\downarrow$ flux is to be expected. The same reasoning holds in Ouagadougou since the ψ_S of the green residential area and the CBD are similar. Thus, radiation from walls is important to $L\downarrow$ variations in the urban canopy layer. This is especially true in Dar es Salaam where temperature and humidity variations are small in contrast to Ouagadougou and Gaborone (Tables 4 and 5).

Another possible explanation of the intra-urban variation of $L\downarrow$ is the role of intra-urban

variations of TSP (Tapper, 1984). Highest concentrations of TSP were not found, as might be expected, in the CBD but rather in the traditional areas of Ouagadougou and Gaborone and in the green traditional area of Dar es Salaam. In this case, the status of the road network seems to be crucial; the majority of all roads are unpaved in the areas of highest concentrations. The most polluted areas are also where most people reside, especially in Ouagadougou and Gaborone. These results contradict the results presented for Hong Kong which showed a low concentration of TSP in residential areas due to low traffic flow (Chan et al., 2001). The traffic flows in the residential areas are also low in the three cities studied. However, TSP concentrations derived from the unpaved streets are greater compared to those originating from combustion processes. This is especially true for the sub-Sahel Africa (Ouagadougou) where proximity to the Sahara desert and the dusty Harmattan winds is related to high concentrations of particles (Miscolczi et al., 1997).

5.2 'Observed' emissivities and differences

From an urban–rural perspective, Fig. 4 showed that the average observed atmospheric emissivity is higher, by approximately 0.03, in the rural areas of all cities compared to the urban areas. Nunez et al. (2000) found the same higher rural emissivity in Göteborg, Sweden. They explained their results in terms of rural inversions that increase apparent sky emissivity. However, in Dar es Salaam, Ouagadougou and Gaborone, the higher rural value of around 0.03 is evident at all times (morning, noon and night) although rural inversions are highly unlikely during the day in the Tropics. This is also evident in the mean diurnal time series (Fig. 5). The choice of wall surface temperatures used in Eq. 4 can partly explain the lower urban values. The effect of sunlit or shaded wall surfaces is not considered in this analysis. However, it should be remembered that solar angles are high in the Tropics with the effect that it is the roofs rather than the walls that are heated during the day. Although urban wall temperatures are higher than the urban air temperature, the urban/rural air temperature difference is small or even negative.

Comparing observed and modelled sky emissivities for all cities (Fig. 6) show that the Prata emissivity formula overestimates in all urban areas in Dar es Salaam and Gaborone, but to a lesser extent in Ouagadougou. There is also a diurnal pattern of sky emissivity that is convincing in all cities, both urban and rural areas (Figs. 5–7). Similar patterns were found in Australia (Paltridge, 1970), Arizona (Idso, 1972) and Spain (Alados-Arboledas and Jimenez, 1988; Alados-Arboledas, 1993). This is explained as an artifact of the calculations since the actual incoming longwave radiation is a result of the vertical properties of the atmosphere while the calculation formulas have surface data as input. The result is that inversions during the night result in temperatures which are lower at the surface than the warm and moist air aloft, and during the day the intense heating results in a superadiabatic lapse rate near the ground and too high a value is input into the formula, resulting in underestimation of the downwelling radiation at night and an overestimation during the day. Alados-Arboledas and Jimenez (1988) found a day–night difference of the apparent sky emissivity of 0.06, i.e. about 10% of the sky emissivity. The day–night difference they calculated in Spain is somewhat smaller than has been found in the present study (0.08). They proposed a sine function to correct for the diurnal lapse rate variation. Due to the observation hours in the present study only the noon calculations were corrected.

5.3 Modelled longwave radiation in urban areas

The correction of the apparent sky emissivity that varies over the day was incorporated in the modeling of urban $L\downarrow$ (i.e. noon emissivities were reduced by 0.04). Together with a single reflection of longwave radiation, as suggested by Harman et al. (2004), this gave satisfactory results ($R^2 = 0.88$). This is a strong indication that factors governing $L\downarrow$ in previous, mid latitude studies, also apply in the Tropics.

The model performs best in Ouagadougou which is somewhat surprising given the large TSP concentrations observed. The results from Dar es Salaam (50 m a.s.l.) and Gaborone (1000 m a.s.l.) yield the same explained variances and overestimation of $L\downarrow$. Izioman et al. (2003)

suggested that clear sky emissivity models should perform less well at higher altitudes, but this was not found in the present study.

At the intra-urban scale, the model performs best in the CBD areas ($R^2 = 0.90$) followed by the traditional residential areas and the green residential areas. The slope of the best fit lines are similar, so the model works acceptably well for all land uses despite the large range of materials, sky view factors, and other factors implicit in the urban mosaic. This is an advantage for future modeling. The same is true regarding time of the day. The strong insolation in the Tropics could easily be imagined to yield large discrepancies between sunlit and night hours but this does not seem to be the case. This shows that the diurnal variation of apparent sky emissivity is an important factor to correct for in models.

5.4 The influence of particles

Strangely, the multiple regression (Table 4) resulted in no or weak covariance between $L\downarrow$ and TSP, not even in highly polluted Ouagadougou. A correlation analysis showed that TSP does not covary with any other parameters indicating that the possible influence of particles is not masked.

Aerosol forcing is only acting in the 8–13 μm window so the effect of the aerosol emissivity is reduced to about 0.32 of a full radiator (Dalrymple and Unsworth, 1978). Thus, the effect of aerosols is diminished and consequently it is not included in any of the emissivity formulas. However, the calculations by Claquin et al. (1998) show that the massive dust loading in Sahara can result in a forcing of $48\,\mathrm{Wm^{-2}}$. In the present study, the near-Saharan city of Ouagadougou with dust laden air, shows observed emissivities close to that calculated (Fig. 6) while the other two cities, with cleaner air, have observed emissivities that are 0.05 lower than calculated. It is puzzling that there is no statistical relationship between the observed-modeled emissivity difference and the level of TSP. This can be explained by the diurnal variation of TSP. High daytime wind speeds generate intensive shear, high-reaching dust cloud and small surface concentration, while low wind speeds during the night allow particles to sink and, as a result, the concentration close to the ground will increase. In spite of the differences in TSP concentration near the surface, the mass of particles and the optical depth in a vertical column is about the same both day and night. An elevated dust layer and/or thin and non-visible cirrus clouds can explain higher observed $L\downarrow$ in Ouagadougou. Elevated dust layers have been shown to exist over the Canary Islands at altitudes of 1–5 km (Powell et al., 2000).

In some cases daytime maxima higher then that calculated have been reported – in Ontario, Canada (Rouse et al., 1973; Arnfield, 1979), Los Angeles (Ackerman, 1977) and Christchurch, New Zealand (Tapper, 1984). Daytime heating by absorption of shortwave radiation was suggested as an explanation. The difference between these cities and those mentioned in section 5.2 is the origin of the aerosols. Tapper (1984) used smoke concentration in his analysis, and smoke is likely to be an important part of the TSP in sites in Ontario, Los Angeles and Christchurch. The three African cities and the other sites mentioned in Section 5.2 have soil derived suspended particles. The albedo of the soil particles is much lower than the albedo of soot and thus the ability to absorb shortwave radiation and emit IR-radiation is much lower. The emissivity of sand, silt and clay is also lower (about 0.7 (Omega, 2004)) compared to soot (0.95).

From this perspective, large or even extreme concentrations of TSP, which potentially have a large effect on the climate, could be another factor setting the Tropical urban climate apart from that of the mid latitudes. Some authors claim that particles have a considerable impact in the Tropics (Miskolczi et al., 1997; Claquin et al., 1998). In the present study the dust laden air in Ouagadougou gives an observed-modelled emissivity difference that is about 0.05 higher than in the other cities, which corresponds to an increase of the incoming longwave radiation of about $20\,\mathrm{Wm^{-2}}$ due to aerosols.

6. Conclusions

This study has shown that Dar es Salaam has the largest $L\downarrow$ flux followed by Ouagadougou and Gaborone. Temperature, as a function of latitude, is an important explanatory variable. Sky-view factors and the emissivities of the sky obstructions are important controls on intra-urban

differences. Clear diurnal patterns in observed sky emissivity, that are not site specific, also are documented. Modelling $L\downarrow$ with diurnal patterns incorporated, yield good results for all land uses in all cities at all times. Consequently, we propose that the model can be applied to African cities broadly with satisfactory results at any time if the sky emissivity is corrected for its diurnal variation.

The influence of suspended particles shows unexpected results. The residual (difference between modelled and observed $L\downarrow$) did not show any relationship with TSP, despite the large concentrations observed, especially in Ouagadougou. A possible explanation might be that soil derived dust shows a considerable diurnal variation near the ground, but the mass of particles in the vertical air column and the optical depth are about the same both day and night. However, it was shown that the difference between observed and modelled ε_{sky} is positive in Ouagadougou while negative in both Dar es Salaam and Gaborone, suggesting that a heavy dust laden atmosphere (as in Ouagadougou) does increase observed ε in relation to modelled ε.

Overall $L\downarrow$ can be modelled using factors that have known impacts in the midlatitudes. The heavy particle load at some locations could provide a physical background for a large change in the longwave radiation balance. However, with pollution of natural origin close to the surface, our results suggest no evident $L\downarrow$-enhancing effect.

Acknowledgements

This project is financially supported by the Swedish International Development Cooperation Agency (Sida). We would like to thank the Physics Departments of University of Dar es Salaam and University of Botswana. Thanks are also due to Tanzania Meteorological Agency, Botswana Meteorological Services and Direction de la Météorologie Nationale, Burkina Faso.

References

Ackerman TP (1977) A model of the effect of aerosols on urban climates with particular applications to the Los Angeles Basin. J Atmos Sci 34: 531–547

Aida M, Yaji M (1979) Observations of atmospheric downward radiation in the Tokyo area. Bound-Layer Meteor 16: 453–465

Aida M (1982) Urban albedo as function of the urban structure – a model experiment. Bound-Layer Meteor 23: 405–413

Alados-Arboledas L, Jimenez JI (1988) Day–night differences in the effective emissivity from clear skies. Bound-Layer Meteor 45: 93–101

Alados-Arboledas L (1993) Estimation of hourly values of downward atmospheric radiation under cloudless skies during day- and night-time conditions. Theor Appl Climatol 48: 127–131

Arnfield AJ (1979) Evaluation of empirical expressions for the estimation of hourly totals of atmospheric longwave emission under all sky conditions. Quart J Roy Meteor Soc 105: 1041–1052

Arnfield AJ (1982) An approach to the estimation of the surface radiative properties and radiation budgets of cities. Phys Geogr 3: 97–122

Brunt D (1932) Notes on radiation in the atmosphere. Quart J Roy Meteor Soc 58: 389–420

Brutsaert W (1975) A derivable formula for longwave radiation from clear skies. Water Resour Res 11: 742–744

Chan LY, Kwok WS, Lee SC, Chan CY (2001) Spatial variation of mass concentration of roadside suspended particulate pollution in metropolitan Hong Kong. Atmos Environ 35: 3167–3176

Claquin T, Schulz M, Balkanski Y, Boucher O (1998) Uncertainties in assessing radiative forcing by mineral dust. Tellus 50B: 491–505

Cohen B (2004) Urban growth in developing countries: a review of current trends and a caution regarding existing forecasts. World Devel 32(1): 23–51

Dalrymple GJ, Unsworth MH (1978) Longwave radiation at the ground: IV. Comparison of measurements and calculation of radiation from cloudless skies. Quart J Roy Meteor Soc 104: 989–997

Diallo M (2004) Regional conference on the suppression of lead in gasoline in Sub-Saharan Africa. http://www.cleanairnet.org/ssa/1414/articles-36194_Diallo_pdf.pdf, accessed October 27, 2004

Estournel C, Vehil R, Guedalia D, Fontan J, Druilhet A (1983) Observations of modeling of downward radiative fluxes (solar and infrared) in urban/rural areas. J Climate Appl Meteor 22: 134–142

Fenger J (1999) Urban air quality. Atmos Environ 33: 4877–4900

Finch JW, Best MJ (2004) The accuracy of downward short- and long-wave radiation at the earth's surface calculated using simple models. Meteorol Appl 11: 33–39

Garratt JA (1992) Extreme maximum land surface temperatures. J Appl Meteor 31: 1096–1105

Grimmond CSB, Potter SK, Zutter HN, Souch C (2001) Rapid methods to estimate sky-view factors applied to urban areas. Int J Climatol 21: 903–913

Harman IN, Best MH, Blecher SE (2004) Radiative exchange in an urban street canyon. Bound-Layer Meteor 10: 301–316

Holmer B, Eliasson I (1999) Urban-rural vapour pressure differences and their role in the development of urban heat islands. Int J Climatol 19: 989–1009

Holmer B, Postgård U, Eriksson M (2001) Sky view factors in forest canopies calculated with IDRISI. Theor Appl Climatol 68: 33–40

Idso SB, Jackson RB (1969) Thermal radiation from the atmosphere. Geophys Res Lett 74: 5397–5403

Idso SB (1972) Systematic deviations of clear sky atmospheric thermal radiation from predictions of empirical formulae. Quart J Roy Meteor Soc 98: 399–401

Idso SB (1981) A set of equations for full spectrum 8- to 14-μm and 10.5- to 12.5-μm thermal radiation from cloudless skies. Water Resour Res 74: 5397–5403

Izioman MG, Mayer H, Matzarakis A (2003) Downward atmospheric longwave irradiance under clear and cloudy skies: measurement and parameterization. J Atmos Sol-Terr Phy 65: 1107–1116

Jauregui E (1999) Tropical urban climatology at the turn of the century. Proc. of the 15th International Congress of Biometeorology & International Conference on Urban Climatology, ICUC 6.2

Jayaratne ER, Verma TS (2001) The impact of biomass burning on the environmental aerosol concentration in Gaborone, Botswana. Atmos Environ 35: 1821–1828

Kimaryo JL (1996) Urban design and space use – a study of Dar es Salaam city centre. Department of building functions analysis, School of Architecture, Lund University, Sweden, 240 pp

Kipp & Zonen (2002) Instruction manual for CG 1 pyrgeometer. Kipp & Zonen P.O. Box 507, Röntegenweg 1 Delft, Netherlands

Mbuligwe SE, Kassenga GR (1997) Automobile air pollution in Dar es Salaam, Tanzania. Sci Total Env 199: 227–235

Miskolczi F, Aro TO, Iziomon M, Pinker RT (1997) Surface radiative fluxes in Sub-Sahel Africa. J Appl Meteor 36: 521–530

Newton T (1999) Energy balance fluxes in a subtropical city: Miami FL. M.S. thesis, Dept. of Geography, University of British Columbia, Vancouver, BC, Canada, 140 pp. [Available from T. Oke at toke@geog.ubc.ca.]

Nunez M, Eliasson I, Lindgren J (2000) Spatial variations of incoming longwave radiation in Göteborg, Sweden. Theor Appl Climatol 67: 181–192

Offerle B, Grimmond CSB, Oke TR (2003) Parameterization of net all-wave radiation for urban areas. J Appl Meteor 42: 1157–1173

Offerle B, Jonsson P, Eliasson I, Grimmond CSB (2005) Urban modification of the surface energy balance in the West African Sahel: Ouagadougou, Burkina Faso. J Climate 18: 3983–3995

Oke TR (1997) Urban environments. In The Surface Climates of Canada. Montreal, Canada: McGill-Queen's University Press, 369 pp

Oke TR (1987) Boundary layer climates. Cambridge, UK: Routledge, University Press, 435 pp

Oke TR, Fuggle RF (1972) Comparison of urban/rural counter and net radiation at night. Bound-Layer Meteor 12: 290–308

Omega (2004) Emissivity of Common Materials, http://www.omega.com/literature/transactions/volume1/emissivityb.html, accessed October 7, 2004

Paltridge GW (1970) Day-time long-wave radiation from the sky. Quart J Roy Meteor Soc 96: 645–653

Rouse WR, Noad D, Cutcheon J (1973) Radiation, temperature and atmospheric emissivities in a polluted urban atmosphere at Hamilton, Ontario. J Appl Meteor 12: 798–807

Padmanabhamurty B, Bandopadhyay D (1994) Radiation balance in a tropical city – Delhi (India). Bound-Layer Meteor 70: 197–210

Powell DM, Reagan JA, Rubio MA, Erxleben WH, Spinhirne JD (2000) ACE-2 multiple angle micro-pulse lidar observations from Las Galletas, Tenerife, Canary Islands. Tellus Ser B 52: 652–661

Prata AJ (1996) A new long-wave formula for estimating downward clear-sky radiation at the surface. Quart J Roy Meteor Soc 122: 1127–1151

Swinbank WC (1963) Longwave radiation from clear skies. Quart J Roy Meteor Soc 89: 339–348

Tapper NJ (1984) Prediction of the downward flux of atmospheric radiation in a polluted urban environment. Aus Meteorol Mag 32: 82–93

Trewartha GT (1982) The earth's problem climates. London, UK: The University of Wisconsin Press, 239 pp

United Nations (2004) World urbanization prospects: the 2003 revision. United Nations, New York

Woodlock J (1974) World climatology – an environmental approach. Whitslake, UK: Edward Arnold Publishers Ltd., 330 pp

World Bank (1996) Rural energy and development: improving energy supplies for two billion people. Washington, D.C., USA: The World Bank, 26 pp

Worldclimate (2005) Mean monthly temperature and precipitation of world cities, http://www.worldclimate.com, accessed March 15, 2005

Authors' addresses: P. Jonsson (e-mail: pelle@gvc.gu.se), I. Eliasson, B. Holmer, Urban Climate Group, Physical Geography, Göteborg University, P.O. Box 460, SE-405 30 Göteborg, Sweden; C. S. B. Grimmond, Environmental Monitoring and Modelling, Department of Geography, King's College London, London WC2R 2LS U.K.